**Report no. changed (Mar 2006): SR-214-UU**

SACLANTCEN REPORT
serial no.: SR-214

*SACLANT UNDERSEA RESEARCH CENTRE*

*REPORT*

# Effects of intrinsic medium inhomogeneities on long-range acoustic transmission

H.G. Schneider

October 1993

**Report no. changed (Mar 2006): SR-214-UU**



Page count for SR-214 (excluding Covers and Data Sheet)

| Pages | Total |
|---|---|
| i–vi | 6 |
| 1–9 | 9 |
| | 15 |

SACLANT Undersea Research Centre
Viale San Bartolomeo 400
19138 San Bartolomeo (SP), Italy

tel: 0187 540 111
fax: 0187 524 600
telex: 271148 SACENT I

NORTH ATLANTIC TREATY ORGANIZATION

Report no. changed (Mar 2006): SR-214-UU



# Effects of intrinsic medium inhomogeneities on long-range acoustic transmission

H.G. Schneider

The content of this document pertains to work performed under Project 19 of the SACLANTCEN Programme of Work. The document has been approved for release by The Director, SACLANTCEN.

John Foxwell

John H. Foxwell
Director

intentionally blank page

**Effects of intrinsic medium inhomogeneities on long-range acoustic transmission**

H.G. Schneider

**Executive Summary:** In the deep sound channel transmission ranges of 1000 km may be achieved at frequencies of a few hundred hertz. For a single transmission the arrival structure of the wavefronts may be measured as a function of time and uniquely related to ray arrivals. These characteristics are used in long range surveillance as well as in tomographic experiments to estimate changes in the environment. In modelling such propagation a deterministic ray-theory approach is normally used which cannot explain the vertical extension of the measured arrival structure into the 'forbidden' region, i.e. the extension into greater depths than the ray-theoretical turning point depth. This is not a penetration into a classical shadow zone, since energy will be arriving at that depth, but not in the time interval under consideration.

A possible explanation of this effect is presented here by assuming an intrinsic stochastic variability of the sound speed which is too small to disturb the main ray paths, but sufficiently large to scatter energy into the 'forbidden' region. This assumption is substantiated by a generic model based on stochastic ray tracing. The effects modelled are of the correct order of magnitude but more exact evaluations cannot be made because of missing oceanographic information.

This type of experimental result could be used to estimate several missing oceanographic quantities. In the present approach only the diffusion constant may be deduced. Determination of additional quantities will require the development of an appropriate methodology.

intentionally blank page

**Effects of intrinsic medium inhomogeneities on long-range acoustic transmission**

H.G. Schneider

**Abstract:** Duda et al. [J. Acoust. Soc. Am. **92**(2), 939–955, 1992] have measured wavefront arrival times over a 1000 km track in the Pacific. In modelling the propagation they use a WKBJ-based approch in the ray-theory limit which cannot explain the vertical extension of the measured arrival structure into the shadow zone, i.e. into depths greater than the ray-theoretical turning point depth. A possible explanation of this effect is presented here by assuming an intrinsic stochastic variability of the sound speed which is too small to disturb the main ray paths but sufficiently large to deviate energy into the shadow zone. This assumption is substantiated by a generic model based on stochastic ray tracing. The effects modelled are of the correct order of magnitude but more exact evaluations cannot be made because of missing oceanographic information. However, this type of experimental result could be used to estimate the missing oceanographic quantities if a more detailed methodology were developed.

**Keywords:** propagation modelling ∘ ray tracing ∘ shadow zone

# Contents

# 1
# Introduction

Duda et al. [1] and Howe et al. [2] have presented extensive measurements and an analysis of wavefront arrivals in the Pacific to examine wavefront fluctuations. In their analysis they use an acoustic propagation code based on the ray limit of the WKBJ approximation which is used to identify arrivals in terms of multiple ray cycles. In their Fig. 3 [1], which is reproduced here as Fig. 1, the arrival times of a single pulse at 1000 km range are displayed for receivers at depths from the surface down to 3000 m. Figure 1a shows their predicted result and Fig. 1b, the intensity measurement exceeding a threshold. Two items are noteworthy, first there are theoretical arrivals on the sound channel axis which arrive later than those in the experimental data, and second, the arrival structure in the experimental data extends to greater depths than in the prediction. This latter difference has already been discussed during a preliminary presentation [2] of the data. It was then suggested by this author that these differences might be due to energy being diverted into that region by small inhomogeneities in the sound-speed structure. This is exactly the point which will be substantiated in this report.

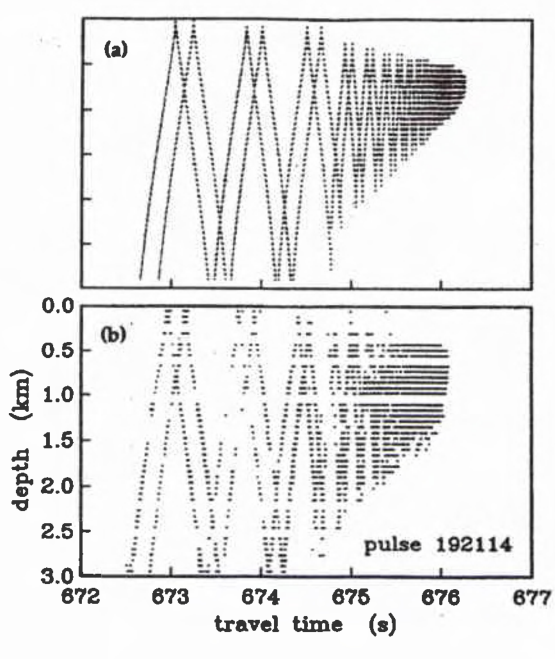


**Figure 1** *From Duda et al. [1]. Wavefront arrival times versus depth for a transmission range of 1000 km in the Pacific. (a) Predicted result based on a ray approach; (b) Measured arrival times.*

# 2
# Method

In almost any sound propagation experiment the interest focuses naturally on the propagation characteristics of the high-energy arrivals, and the low-energy arrivals are either masked or contribute only a negligible amount. The low-energy arrivals often become visible only if they are sufficiently separated from the main path of propagation either in space or time and only if the background noise is sufficiently low. A shadow zone, as in this experiment, constitutes an ideal location for their detection. The shadow zone is here defined by the envelope of the turning point depths of the subsequent ray arrivals in time. Energy may be carried into this region by either diffraction or scattering, or both simultaneously.

The diffraction will not be discussed in detail, but from a full wave theory example the influence of diffraction can be inferred by comparison with the ray-theoretical approach.

To study the influence of intrinsic sound inhomogeneities we apply the ray-diffusion concept [3] which has been sucessfully applied in a similar case [4].

# 3
# Generic example

### 3.1. NO VARIABILITY

As a generic example the Munk profile

$$c(z) = c_0[1 + \epsilon\ (\ e^{-\eta(z)} - \eta(z) + 1)] \tag{1}$$

is used with the following parameters:

$$\eta = -2(z - z_0)/B, \qquad \epsilon = (B/2) \times 1.14 \times 10^{-2},$$
$$c_0 = 1480 \text{ m/s}, \qquad z_0 = B = 1.3 \text{ km}.$$

For a source depth of 1.3 km and a propagation range of 1000 km the wavefront arrivals due to a ray-tracing code [3,4] are as given in Fig. 2. A single profile was assumed for the entire track and an infinite bottom loss was applied, limiting the propagation to refracted arrivals only. A threshold of 110 dB transmission loss was chosen, so that with a source level of 192 dB the received signal would equal the reported noise level. (Duda et al. [1] assume spherical spreading for the entire 1000 km track, which seems unrealistic and gives about 20 dB too much loss.) The upper and lower turning points in depth reflect the asymmetry of the sound-speed profile relative to the channel axis. The envelope of the turning points constitutes the shadow zone boundary and the increasing time axis corresponds to decreasing propagation angles.

### 3.2. DIFFRACTION

To estimate the energy being diffracted into the ray-theoretical shadow zone a full wave solution is required. Here the normal-mode program SUPERSNAP is used and the arrival of a pulse at 1000 km is computed via standard FFT techniques. We restrict this analysis to the one turning point which is given in Fig. 2 at a time of 0.66 s and a turning point depth of 3950 m. Figure 3 displays an enlarged version of this area for the normal-mode solution. The centre frequency of 250 Hz was chosen as in the experiment with a bandwitdth of ±40 Hz. As expected, energy can be detected below the ray-theoretical turning point down to about 4025 m which is 75 m or about 12 wavelenths below the ray limit. However, this extension is not sufficient to explain the measured data which extends 400 m below the ray turning points. (The structure to the right is an earlier arrival which wrapped around in this time window.)

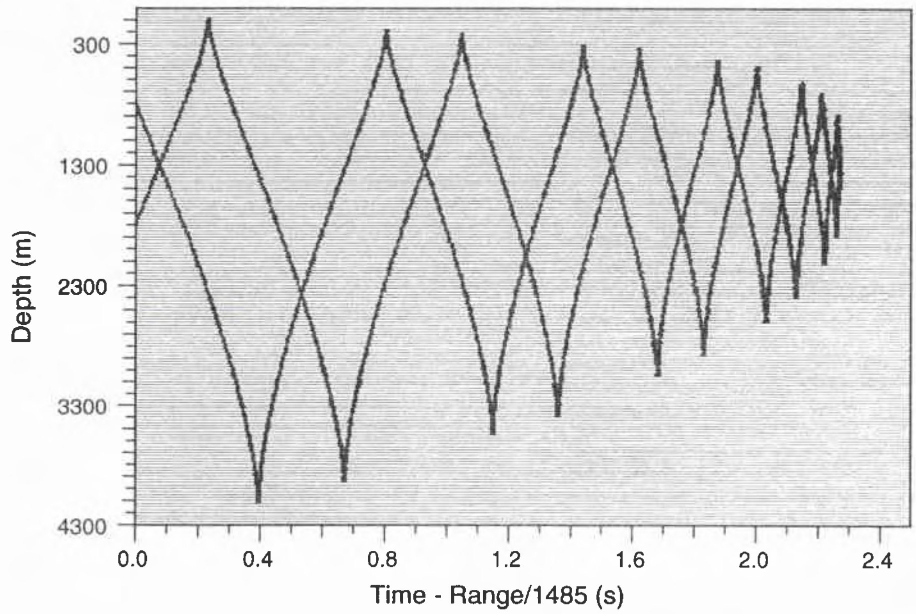


**Figure 2** *Arrival times at 1000 km range due to a single Munk profile with no sound-speed variability. Source depth 1.3 km, reduction speed* $C_r = 1485$ *m/s.*

### *3.3. INTRINSIC SOUND-SPEED VARIABILITY*

To estimate effects of the intrinsic sound-speed variability, a ray-tracing scheme is applied which uses piecewise linear sound-speed gradients versus depth. The main difference from other ray-tracing codes is the evaluation of the energy at a receiver. This is done by simply summing in a vertical receiver window of dimension $dz$ the incoherent ray intensities associated with single rays which penetrate this window. Hence all difficulties usually occurring with ray divergence methods are avoided, but a sufficiently large number of rays has to be traced if this method is to be applied to deep-water acoustics. An insufficient number of rays, or equivalently a too large angular separation at the source, will leave some receiver windows empty. Also the sound-speed profile must be sampled sufficiently finely to avoid large discontinuities in the sound-speed gradients of adjacent depth intervals, otherwise this may lead to errors for the late arrival times.

The intrinsic stochastic variability of the sound speed $\Delta c$ is assumed to be small compared to any sound speed $c(z)$ in the profile. Following Chernov [5] we assume a zero mean process $\overline{\Delta c} = 0$ and define the variance of the index of refraction as $\mu^2 = \overline{(\Delta c/c)^2}$. Further we assume an isotropic background profile $c = c_0$, and a Gaussian correlation function of the stochastic variability $\Delta c$ with correlation length $a_0$. Using the ray diffusion approach in the limit for small angular perturbations results in a Gaussian density for the change in propagation angle $\Delta\phi$ with a standard variation of

$$\sigma_{\Delta\phi} = \sqrt{2Ds}, \qquad D = \sqrt{\pi}\frac{\mu^2}{a_0}, \tag{2}$$

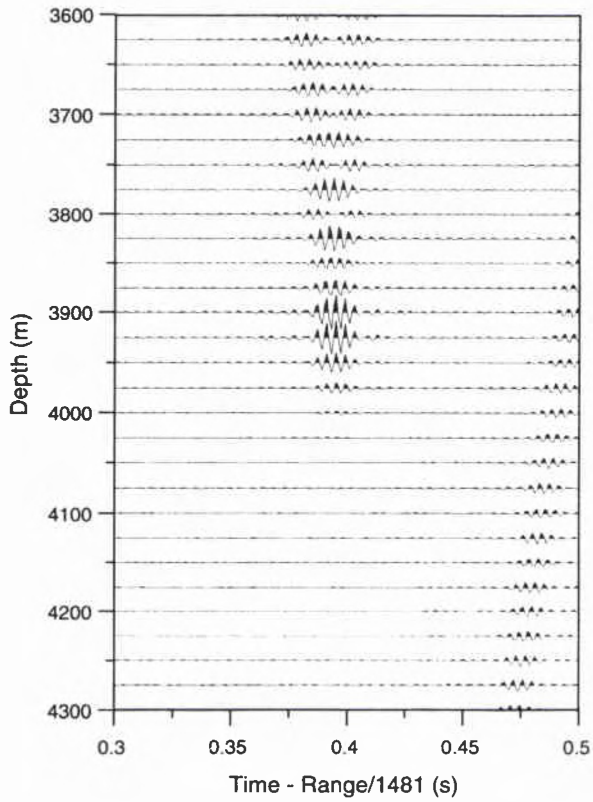


**Figure 3** *Single turning point of a pulse arrival computed with normal modes. Corresponds to the turning points of Fig. 2 at* $t = 0.66$ *s and a depth of 3950 m.*

where $s$ is the path length in the stochastic medium and $D$ the diffusion constant. The small perturbation angle approximation requires that $\sigma_{\Delta\phi} \ll 1$. Obviously the requirement of an isotropic background profile is not met for a canonical deep-water profile. However, if small perturbation angles and short path lengths between scattering events are used, this may still be a reasonable assumption in the vicinity of the sound channel axis where the sound-speed gradient is small.

This diffusion concept is implemented into the ray tracing in the following way. A ray is traced according to the sound-speed profile $c(z)$ from one boundary of a sound-speed layer to the next and the path length is accumulated. The path length between scattering events is controlled by the length $S_{\text{scat}}$. If the path length $s_{\text{s}}$ measured from the last scattering event is within $S_{\text{scat}} \leq s_{\text{s}} \leq 2S_{\text{scat}}$ at some boundary then the propagation angle is changed at that boundary by the random quantity $\Delta\phi$ according to the Gaussian density distribution above. If the path length $s_{\text{s}}$ at the layer boundary is larger than $2S_{\text{scat}}$, the ray segment will be terminated at a path length $S_{\text{scat}}$ from the last boundary (i.e. within the layer) and the change of propagation angle is applied there. This provides a certain randomization of the scattering locations without requiring too many additional computations, and limits the path length between scattering events.

The size of the small-scale sound-speed variability is not very well established. Chernov reports data from a depth of 30 to 60 m with $\mu^2 = 5 \times 10^{-9}$ and a mean size of the inhomogeneities of $a_0 = 0.60$ m. This leads to $\Delta c_{\rm rms} = 0.1$ m/s and $D = 1.5 \times 10^{-8}$ m$^{-1}$.

In the deeper parts of the ocean the variability is certainly smaller and choosing $D = 3 \times 10^{-10}$ m$^{-1}$ would correspond to $\Delta c_{\rm rms} = 0.3$ m/s or $\Delta T_{\rm rms} = 0.07\,°$C with a correlation length $a_0 \approx 600$ m. For a maximum path length $s = 2S_{\rm scat} = 4000$ m between scattering events the rms angular variation is $\sigma_{\Delta\phi} = \sqrt{2Ds} = 0.09°$. Because the diffusion approximation requires an isotropic background profile the scattering has been restricted to path segments in the depth region from 900 m to 1750 m, i.e. where the sound-speed gradient is sufficiently small.

These parameters lead to the arrival pattern in Fig. 4. The horizontal bars indicate the depth of the turning points in the deterministic case which is displayed in Fig. 5 as an enlarged section of Fig. 2. The energy at the turning points of the wavefronts extends in the stochastic case about 250 m deeper than in the deterministic one. This is the same order of magnitude as the differences in Fig. 1. Obviously the main wavefronts remain undisturbed and the scatter is only slightly increased. Further the extension of energy to larger depths does not result in a significant time spread or time delay, which is remarkable since this implies that a bundle of rays with different angles arrives at different depths within the resolution cell of 0.005 s. At the upper shadow zone, where the sound-speed gradient is larger, the illumination due to scattering does not extend so deeply into the shadow.

A larger diffusion constant will increase the scatter around the wavefronts because the ray may arrive with a displacement in depth, and energy will be carried even further beyond the deterministic turning point depth of the ray.

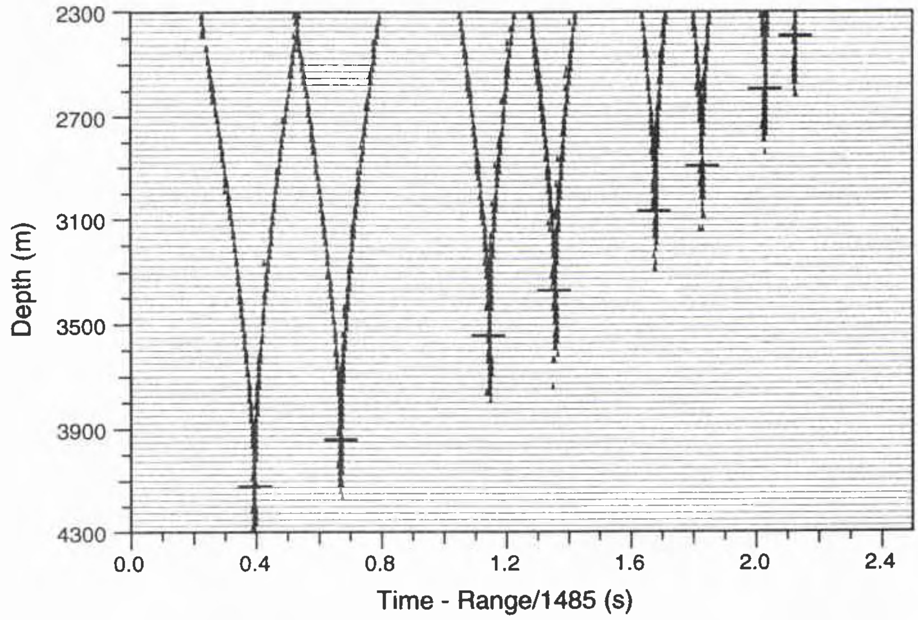


**Figure 4** *Arrival times at 1000 km range due to a single Munk profile with sound-speed variability: diffusion constant* $D = 3 \times 10^{-10}\ m^{-1}$, $S_{\mathrm{scat}} = 2000\ m$. *The horizontal bars indicate the turning point depths of Fig. 5. Source depth 1.3 km, reduction speed* $C_r = 1485\ m/s$.

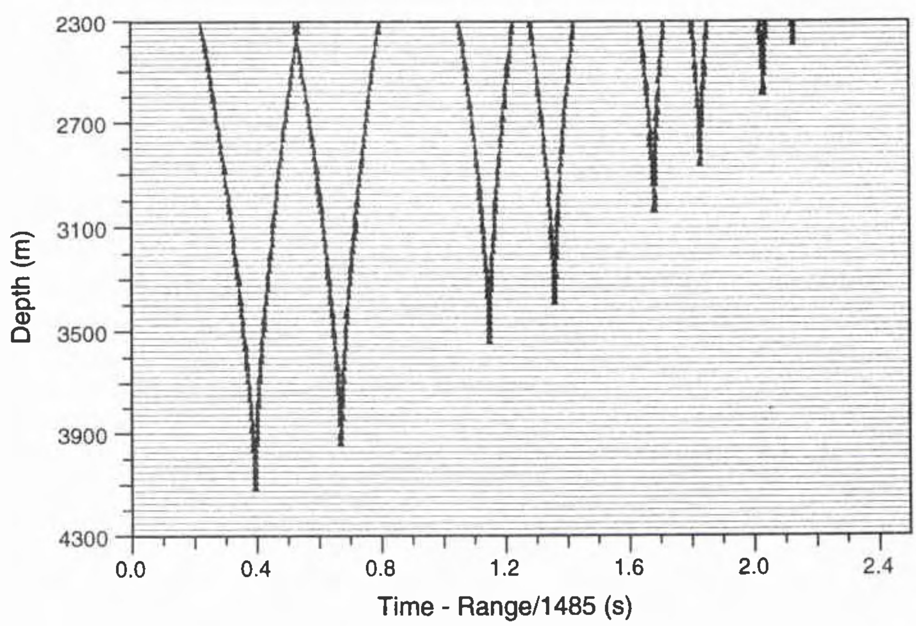


**Figure 5** *Expanded part of Fig. 2. Arrival times at 1000 km range due to a single Munk profile with no sound-speed variability. Source depth 1.3 km, reduction speed* $C_r = 1485\ m/s$.

# 4

# Conclusion

By using a simple stochastic ray tracing scheme it has been shown that small stochastic sound-speed variations divert energy into the ray-theoretical shadow zone. This intrinsic variability illuminates regions even beyond the shadow zone boundary where diffraction effects are important, but it leaves the remainder of the arrival pattern unchanged. The extension of energy into the shadow zone is a function of the sound-speed gradient and the sound-speed variability.

This provides a possible explanation for the shadow zone illumination in the experimental results of Duda et al. [1] and Howe et al. [2], since the computational result describes the finding within the correct order of magnitude. Proper modelling would require a better description of the nature of the intrinsic sound-speed variation in terms of variance, correlation lengths and variation with depth and range.

If the explanation offered is the dominant cause of this acoustic phenomenon, then this type of experimental result has the potential to determine the missing oceanographic quantities. In the present approach, however, only the diffusion constant may be deduced. To obtain more detailed information on the variance and correlation lengths of the intrinsic stochastic variability an appropriate methodology would need to be developed.

# References

[1] Duda, T.F., Flatté, S.M., Colosi, J.A., Cornuelle, B.D., Hildebrand, J.A., Hodgkiss, W.S., Worcester, P.F., Howe, B.M., Mercer, J.A. and Spindel, R.C. Measured wavefront fluctuations in 1000-km pulse propagation in the Pacific Ocean. *Journal of the Acoustical Society of America*, **92**, 1992: 939–955.

[2] Howe, B.M., Mercer, J.A., Spindel, R.C., Worcester, P.F., Hildebrand, J.A., Hodgkiss, W.S., Duda, T.F. and Flatté, S.M. SLICE 89: A single slice tomography experiment. *In:* Potter, J. and Warn-Varnas, A., *eds.*, Ocean Variability and Acoustic Propagation. Dordrecht, Kluwer: 1991, pp. 81–86. [ISBN 0-7923-1079-9]

[3] Schneider, H.G. Excess sound propagation loss in a stochastic environment. *Journal of the Acoustical Society of America*, **62**, 1977: 871–877.

[4] Schneider, H.G. Average sound intensities in randomly varying sound-speed structures. *In:* Potter, J. and Warn-Varnas, A., *eds.*, Ocean Variability and Acoustic Propagation. Dordrecht, Kluwer: 1991, pp. 283–292. [ISBN 0-7923-1079-9]

[5] Chernov, L.A. Wave Propagation in a Random Medium. New York, NY, McGraw-Hill, 1960. [LCN 60-11437]

# Document Data Sheet

NATO UNCLASSIFIED

Report no. changed (Mar 2006): SR-214-UU

| | | |
|---|---|---|
| *Security Classification* NATO UNCLASSIFIED | | *Project No.* 19 |
| *Document Serial No.* SR-214 | *Date of Issue* October 1993 | *Total Pages* 15 pp. |

*Author(s)*

H.G. Schneider

*Title*

Effects of intrinsic medium inhomogeneities on long-range acoustic transmission

*Abstract*

Duda et al. [J. Acoust. Soc. Am. **92**(2), 939–955, 1992] have measured wavefront arrival times over a 1000 km track in the Pacific. In modelling the propagation they use a WKBJ-based approch in the ray-theory limit which cannot explain the vertical extension of the measured arrival structure into the shadow zone, i.e. into depths greater than the ray-theoretical turning point depth. A possible explanation of this effect is presented here by assuming an intrinsic stochastic variability of the sound speed which is too small to disturb the main ray paths but sufficiently large to deviate energy into the shadow zone. This assumption is substantiated by a generic model based on stochastic ray tracing. The effects modelled are of the correct order of magnitude but more exact evaluations cannot be made because of missing oceanographic information. However, this type of experimental result could be used to estimate the missing oceanographic quantities if a more detailed methodology were developed.

*Keywords*

propagation modelling, ray tracing, shadow zone

*Issuing Organization*

North Atlantic Treaty Organization
SACLANT Undersea Research Centre
Viale San Bartolomeo 400, 19138 La Spezia, Italy

*[From N. America: SACLANTCEN CMR-426
(New York) APO AE 09613]*

tel: 0187 540 111
fax: 0187 524 600
telex: 271148 SACENT I

NATO UNCLASSIFIED

**Report no. changed (Mar 2006): SR-214-UU**

## Initial Distribution for SR-214

| | |
|---|---|
| *Ministries of Defence* | |
| JSPHQ Belgium | 2 |
| DND Canada | 10 |
| CHOD Denmark | 8 |
| MOD France | 8 |
| MOD Germany | 15 |
| MOD Greece | 11 |
| MOD Italy | 10 |
| MOD Netherlands | 12 |
| CHOD Norway | 10 |
| MOD Portugal | 5 |
| MOD Spain | 2 |
| MOD Turkey | 5 |
| MOD UK | 20 |
| SECDEF US | 60 |
| *NATO Authorities* | |
| NAMILCOM | 2 |
| SACLANT | 3 |
| CINCIBERLANT | 1 |
| COMSUBACLANT | 1 |
| PAT | 1 |
| *SCNR for SACLANTCEN* | |
| SCNR Belgium | 1 |
| SCNR Canada | 1 |
| SCNR Denmark | 1 |
| SCNR Germany | 1 |
| SCNR Greece | 1 |
| SCNR Italy | 1 |
| SCNR Netherlands | 1 |
| SCNR Norway | 1 |
| SCNR Portugal | 1 |
| SCNR Spain | 1 |
| SCNR Turkey | 1 |
| SCNR UK | 1 |
| SCNR US | 2 |
| French Delegate | 1 |
| SECGEN Rep. SCNR | 1 |
| NAMILCOM Rep. SCNR | 1 |
| *National Liaison Officers* | |
| NLO Belgium | 1 |
| NLO Canada | 1 |
| NLO Denmark | 1 |
| NLO Germany | 1 |
| NLO Italy | 1 |
| NLO Netherlands | 1 |
| NLO UK | 1 |
| NLO US | 1 |

| | |
|---|---|
| Total external distribution | 211 |
| SACLANTCEN Library | 10 |
| Stock | 29 |
| Total number of copies | 250 |